Marine Pollution Bulletin, Vol. 45, No. 1-12, 2002, pp 300-310

TWO-LAYERED, 2-D UNSTEADY EUTROPHICATION MODEL IN BOUNDARY-FITTED COORDINATE SYSTEM

K.W.Chau* and Haisheng Jin
Department of Civil & Structural Engineering, Hong Kong Polytechnic University, Hung Hom, Kowloon, Hong Kong.
*fax no: (852) 2334 6389 email: cekwchau@polyu.edu.hk

ABSTRACT

The decline of water quality in Tolo Harbour in recent years is an example of eutrophication. This paper delineates a robust unsteady two-layered, 2-d finite difference numerical model for eutrophication in coastal waters. The modelling is based upon the numerically generated boundary-fitted orthogonal curvilinear grid system and integrated with a hydrodynamic model. It simulates the transport and transformation of nine water quality constituents associated with eutrophication in the waters, i.e. three organic parameters (carbon, nitrogen and phosphorus), four inorganic parameters (dissolved oxygen, ammonia, nitrite + nitrate and orthophosphate), and two biological constituents (phytoplankton and zooplankton). Key kinetic coefficients are calibrated with the field data. The hydrodynamic, pollution source and solar radiation data in the model are real-time simulated. The computational results show that the present model mimic the stratification tendency for eutrophication phenomena during summer time in the Tolo Harbour successfully. The model running time for the long-term simulation is not excessive and it can be run on a microcomputer.

KEYWORDS

Boundary-fitted orthogonal; curvilinear co-ordinate system; eutrophication; finite difference method; numerical model; water quality.

INTRODUCTION

The excessive growth of aquatic plants, both attached and planktonic, to levels that are considered to be an interference with desirable water uses bring about the eutrophication phenomenon. The growth of aquatic plants results from many causes. One of the principal stimulants, however, is an excess level of nutrients such as nitrogen, phosphorus, etc. In recent decades, the eutrophication problem has been increasingly acute all over the world due to the discharge of such nutrients by municipal and industrial sources, as well as in agricultural and urban runoff. It has often been observed that there is an increasing tendency for some water bodies to exhibit increases in the severity and frequency of algae blooms and growth of aquatic weeds apparently as a result of elevated levels of nutrients. (Thomann and Mueller, 1987) The eutrophication problem is one of the most important water quality problems in Europe and much effort and money have been spent on combating it. The problem has been researched extensively, and many studies, including eutrophication control and modelling, etc. have been performed. (Boers and van der Molen, 1993; Cerco and Cole, 1993 Lung et al., 1993)

Until recently, many areas of coastal waters in Hong Kong receive sewage directly from urbanized catchments, as well as waste discharges from domestic, livestock and industrial sources via streams and stormwater runoffs. All these waste discharges carry a heavy loading of the nutrients, nitrogen and phosphorus, that are required for the growth of phytoplankton.

Therefore, most of coastal waters have excessive nutrient contents with high eutrophic potential and the development of algae blooms including red tides. The decline of water quality in Tolo Harbour in recent years is a typical example of eutrophication. There were a total of 89 red tide occurrences in Hong Kong with 39 cases recorded in Tolo Harbour in one single year. (Environmental Protection Department, 1990) The deteriorating conditions in Tolo Harbour had been noted by the government of Hong Kong. Tolo Harbour was declared as the first Water Control Zone in Hong Kong on first of April, 1992 and Statutory Water Quality objectives were established on 18th of June, 1982 (Environmental Protection Department, 1990). Sin and Chau (1992) analyzed the trophic status of Tolo Harbour based on monitoring data, with particular reference to chlorophyll-a, secchi depth, total nitrogen and total phosphorus concentrations. In this paper, a two-layered, two-dimensional eutrophication numerical model, integrated with a hydrodynamic model and using a numerically generated boundary-fitted orthogonal curvilinear coordinate system, is delineated. The long-term simulation results in Tolo Harbour are compared with the field data at different locations in the harbour. In addition, comparison of the results is also made with the results of a depth-averaged, two-dimensional eutrophication model (Chau and Jin, 1999), which employed basically the same algorithm except with a single layer in the whole water depth.

METHOD

This eutrophication model actually describes the balance of mass and energy within an ecosystem. Several physical, chemical, biochemical and biological processes can affect the transport and interaction among the nutrients, phytoplankton, zooplankton, carbonaceous material, and dissolved oxygen in the aquatic environment. Mass and energy transformations are regulated by processes such as growth, respiration, mortality, and decomposition. These in turn are governed by environmental quality parameters such as temperature, toxicity, and nutrient concentrations, etc. The system is highly coupled, as energy and mass balance for individual constituents is invariably linked to several others. The state variables in the surface layer are also related with those in the bottom layer through the interface. (Figure 1)

Here, a system of nine state variables are considered, which are three organic parameters (carbon, nitrogen and phosphorus), four inorganic parameters (dissolved oxygen, ammonia, nitrite + nitrate and orthophosphate), and two biological constituents (phytoplankton and zooplankton). An unsteady two-layered two-dimensional eutrophication numerical model is developed, calibrated and verified for Tolo Harbour, Hong Kong. Ammonia, nitrite + nitrate and orthophosphate are taken as the available nutrients for uptake by the phytoplankton. A 10-year field data set (1981-1990) in Tolo Harbour showed that silicate is plentiful, with the average silicate to inorganic nitrogen ratio being equal to 13.8. In accordance with the Liebig's Law of the Minimum, the growth rate of algae is limited by the essential nutrient that is most scarce in the environment relative to the needs of the organism. As such, silicate is excluded as a limiting nutrient in the model system. (Chau and Sin, 1992)

In addition to the above nine variables, solar radiation intensity, water temperature and salinity which will mainly affect some coefficients and the saturated dissolved oxygen, will be taken as known variables by using the existing historical data set. Figure 2 shows the spatially averaged surface water temperature and daily solar radiation intensity in Tolo Harbour. The eutrophication model, which is a two-layered two-dimensional finite difference numerical model, is coupled to a hydrodynamic model (Chau and Jin, 1995). The water quality variables and transport equations of pollutants solved in the model are defined and derived in a similar way to those of the hydrodynamic model (Chau and Jin, 1995). The coordinate system used, the same as that in the hydrodynamic model, is a numerically generated boundary-fitted orthogonal curvilinear system in order to adapt the complicated boundaries of the interested water body. In addition, a grid "block" technique is employed to tackle the problem resulted from unsteady water boundary in the vicinity of the tidal flats.

The plentiful sources of error in both our structural and measured knowledge of an ecological process make it difficult to select the most correct formulation for a specific process in an ecosystem. The reason for this is the difficulty in obtaining harmonized, regular, high-frequency spatial and temporal field data with reasonable accuracy. The governing equations for two-layered water quality variables could be derived from the partial differential equations describing conservation of mass and momentum of incompressible fluid and conservation of mass of pollutants by integrating vertically over the depth of each layer or over the total depth in areas too shallow for a two-layer representation. A hydrostatic pressure distribution and constant density are assumed. The Boussinesq approximation for turbulent stresses and fluxes (Rodi, 1980) are adopted. In addition, the diffusive exchanges across the water surface and the bed are assumed to be zero. A general differential transport equation can be obtained based upon the boundary-fitted orthogonal curvilinear coordinate system (Chau and Jin, 1995) for two-layered concentration of each state variable. The source term for each water quality variable may represent the reaction kinetics, settling, sediment release, external sources and/or sinks.

In this study, chlorophyll-a is taken as a measure of the gross level of phytoplankton. Phytoplankton decreases due to the overall death or mortality (including the endogenous respiration, zooplankton predation or grazing for diatoms and greens only and non-predatory mortality) and settling to the sediment. It increases due to its growth and its direct source. The growth rate of phytoplankton depends on three principal components: temperature, solar radiation and nutrients. Upon death, all the carbon, nitrogen, and phosphorus contained in the algae biomass is returned to the carbonaceous BOD (CBOD), organic nitrogen and phosphorus pools. However, during respiration, carbon is given off as carbon dioxide rather than CBOD, and through grazing only portion of the organic contents of the algae is returned to the respective organic pools. Through settling, none of the organic cell material is returned to the organic pools except in the sediment.

Zooplankton concentration is represented by the organic carbon equivalence. It grows due to uptake of phytoplankton and direct source and it decreases due to its own respiration, non-predatory mortality, predation by the next level in the food chain, and settling. The growth rate of zooplankton depends on the rate at which the zooplankton feeds on the phytoplankton, the amount of phytoplankton available, zooplankton assimilation efficiency, and efficiency of the conversion of phytoplankton biomass to zooplankton biomass.

Regarding the kinetics of the nitrogen species, ammonia and nitrate are used by phytoplankton for growth. During algae and zooplankton endogenous respiration and non-predatory mortality, a fraction of the cellular nitrogen is returned to the dissolved and particulate organic nitrogen pool. The remaining fraction is recycled to the inorganic pool in the form of ammonia nitrogen and readily available for uptake by other viable algae cells. Organic nitrogen is converted to ammonia at a temperature- and phytoplankton-dependent rate, and ammonia is then converted to nitrate via nitrite (nitrification) at a temperature- and oxygen-dependent rate. Nitrate may be converted to nitrogen gas (denitrification) in the absence of oxygen and at a temperature- and oxygen-dependent rate. Organic nitrogen decreases as it converts to ammonia nitrogen and settles to the sediment, and increases due to recycling of dead algae and zooplankton and direct sources. Ammonia nitrogen increases from recycling of dead phytoplankton and zooplankton, organic nitrogen heterotrophic decomposition and direct sources and decreases by consumption of phytoplankton, and also due to biological oxidation to nitrate via nitrite nitrogen. Nitrite is generally rapidly converted to nitrate and so nitrite and nitrate can be combined. Nitrite + nitrate nitrogen is consumed by phytoplankton, denitrification, and increases due to oxidation of ammonia nitrogen and direct sources.

As phosphorus is considered, dissolved inorganic phosphorus is utilized by phytoplankton for growth, and interacts with particulate inorganic phosphorus via a sorption-desorption mechanism. A fraction of the phosphorus released during phytoplankton and zooplankton endogenous respiration and non-predatory mortality is in the inorganic form and is readily available for uptake by other viable algae cells. The remaining fraction released is in the organic form and must undergo mineralization or bacterial decomposition into inorganic phosphorus before utilization by phytoplankton. Organic phosphorus decreases because of conversion to inorganic phosphorus and settling to the sediment, and increases due to recycling of dead phytoplankton and zooplankton and direct sources. Orthophosphate phosphorus decreases due to the consumption of phytoplankton growth and increases due to recycling of dead phytoplankton and zooplankton, the conversion of organic phosphorus to orthophosphate phosphorus and direct sources.

The long history of applications has focused primarily on the use of biochemical oxygen demand as the measure of the quantity of oxygen-demanding material and its rate of oxidation as the controlling kinetic reaction. This has proven to be appropriate for waters receiving a heterogeneous combination of organic waters of municipal and industrial origin since an aggregate measure of their potential effect is a great simplification that reduces a complex problem to one of tractable dimensions. Thus, organic carbon is represented by carbonaceous biochemical oxygen demand, which decreases due to stabilization through uptake of dissolved oxygen, denitrification and settling to the sediment, and is augmented by recycled phytoplankton and zooplanklon to cell carbon and direct source. The sources of dissolved oxygen are re-aeration from the atmosphere, photosynthetic oxygen production and its direct source, etc. Its internal sinks are oxidation of carbonaceous waste material, oxidation of nitrogenous waste material, oxygen demand of sediments of the water body, use of oxygen for respiration by aquatic plants and zooplankton, etc.

The importance of sedimentary oxygen consumption in the oxygen balance of natural waters has been recognized. Sediment oxygen demand may include oxygen consumption in oxidation of sediment organic carbon and others, for example, dissolved methane and ammonia oxidation reactions, etc. Primary production by phytoplankton in surface waters is a major source of labile organic carbon to coastal sediment. In addition to the external sources of nutrients, the release of nutrients from the sediments may also be important. The impact of sediment nutrient release can be significant and result in continuing eutrophication problems even after point sources have been substantially reduced through control measures. According to relevant in situ analysis on nearly 80 samples from June to October 1998, at five different locations in Tolo Harbour, the sediment releases of nutrient were measured as listed below: organic nitrogen between 6 and 40 mgN/(m^2day); ammonia nitrogen between 18 and 205mgN/(m^2day); nitrite + nitrate nitrogen between -4.43 and 9.16 mgN/(m^2day); organic phosphorus between 0.17 and 1.61 mgP/(m^2day); and orthophosphate phosphorus between 1.45 and 8.90 mgP/(m^2day). In the model, the average values are adopted for computational simplicity.

The above interactions between different state variables are represented by numerical equations and a number of kinetic parameters are used in the eutrophication model. Some typical values and their temperature corrections (θ) come from literatures, while others are calibrated with field data especially for the scenario in the Tolo Harbour. Table 1 shows the names and values of the parameters. A boundary-fitted orthogonal curvilinear coordinate system is employed in the model. Under this system, the gradient type boundary conditions at the bank boundary may be treated easily and accurately. At open boundaries, the concentrations for all water quality variables are specified when water flows into the interested water body, and the normal gradients of the concentrations are specified as zero when water flows out. The initial conditions are obtained by interpolating the corresponding boundary conditions at starting time. Actually, initial conditions can be specified with any value because repeated applications of the model show that the impact of inaccurate initial conditions on the output disappears quickly.

It should be emphasized that during the following simulation of Tolo Harbour, tidal elevations at the open boundary, which are calculated from a harmonic analysis using 42 tidal constituents of a long series of tidal observations at a nearby tide gauge at Kau Lau Wan, are specified as the open boundary condition.

A staggered grid system, in which the nodes for velocities and water surface elevation (and scalar variables) do not coincide with each other, is adopted. Control-volume formulation is employed to discretize the differential equations governing water quality processes. (Patankar, 1980) The discretization equation obtained in this manner expresses the conservation principle for the variable in the finite control volume, just as the differential equation expresses it for an infinitesimal control volume. The algebraic set is solved by Tri-Diagonal Matrix Algorithm with Alternating Direction Iteration, for the upper layer first and then for the lower layer. The procedure of the solution at a given time step is as follows: the hydrodynamic model is called first, and then the equations for phytoplankton, zooplankton, organic nitrogen, ammonia nitrogen, nitrite + nitrate nitrogen, organic phosphorus, orthophosphate phosphorus, carbonaceous BOD and dissolved oxygen are solved in sequence. The above procedure is carried out step by step and the time varying two-layered water quality process will be obtained.

RESULTS AND DISCUSSION

Calibration and verification of the model were effected using the long-term time-series field data in Tolo Harbour, Hong Kong (Figure 3). The computational grid system is the same as that in the hydrodynamic model (Figure 4). A boundary-fitted orthogonal curvilinear grid system with a total of 580 grid cells is employed. Longitudinal grid size is about 110 - 710 m and transverse size about 60 - 530 m. The pollution sources entering the harbour are comprised of those from five main tributaries and those from outfalls of two sewage treatment plants at Shatin and Taipo, which are unsteady and are taken as point-sources in the model. Pollutant source loadings from each stream have averaged BOD_5 between 200 – 600 kg/day, total nitrogen 100 – 400 kg/day and total phosphorus 400 – 1600 kg/day. Non-point-sources are not available and so they are not considered in the simulation. A two-year simulation with a time step of 5 minutes, including running of the hydrodynamic model simultaneously, takes about 19.5 hours on a pentium IBM compatible microcomputer.

Tolo Harbour waters are weakly mixed in the summer with an obvious two-layered feature. Serious oxygen depletion and anoxic condition may appear in the bottom layer even when the surface water is still well oxygenated. During the winter, Tolo Harbour waters are vertically well mixed and stratification almost diminishes. As a result, vertically uniform water quality conditions may be attained. Figure 5 shows the layered-averaged, long-term time-series comparisons of results computed and measured at TM6 in Tolo Harbour during 1985-86, while Figure 6 shows the results and comparisons obtained with a depth-averaged model. Two quantities at 7:00 am and 7:00 pm of the water quality parameters, which almost represent the minimum and maximum of algal biomass for one day due to the effect on the growth, are displayed. The major ticks on the time abscissa in these figures designate year and the minor ticks indicate month. Figure 7 shows the chlorophyll-a and dissolved oxygen computed and measured at different locations in Tolo Harbour during 1988-90, while Figure 8 shows the results obtained with a depth-averaged model. It can be seen that the two-layered model reproduces well the stratification tendency in all the water quality state variables while the depth-averaged model does not do so.

The oscillation on model predictions for chlorophyll-a and other variables reflects the complexity of ecological processes. It may be caused by several reasons, including the considerable variation of light intensity, pollutant loadings, tidal flow, density stratification, water temperature and salinity. Besides, many of these parameters are closely linked to and governed by one another. A particular difficulty in calibrating the model is that the observations were instantaneous values from discrete volumes of water, whereas the predictions are of average values for the substantial volumes of water in the grid cells as described above. Therefore a reasonable test of the validity of the numerical model appears to be that its predictions should agree closely with the central trend of the observations. From that viewpoint, the computational results by the present eutrophication model mimic the field data measured in the Tolo Harbour fairly well, i.e., the present eutrophication model could represent reasonably the algae growth dynamics and water quality time-variations, including layered-averaged chlorophyll-a, dissolved oxygen, carbonaceous BOD, organic nitrogen, ammonia, nitrite + nitrate, organic phosphorus, orthophosphate and zooplankton concentrations, in the harbour.

It is found that water quality in the Tolo Channel is better than that in the inner harbour. The water in the inner harbour has been seriously polluted due to substantial pollution loads and poor tidal flushing. The algae growth dynamics relates to multiple factors, including available nutrients, water temperature, solar radiation, zooplankton grazing, tidal flushing and so on. During January and February, the water temperature is low and the solar radiation is weak, low chlorophyll-a concentration and saturated DO appear to be characteristic of the water body. During the spring and early summer, starting from March, the water temperature rises and the solar radiation intensifies, the chlorophyll-a concentrations can attain their annual maximum and the nutrients are rapidly depleted by the algae bloom. Meanwhile, the DO maintains a super-saturated period due to photosynthesis and then rapidly decreases because of the activity of settled algae carbon as sediment oxygen demand and reaches its annual minimum near June. From later summer till December, the lower chlorophyll-a concentration is maintained and the DO is restored gradually to its saturated status. The nutrients are also increased gradually due to less utilization by algae during that period.

It can also be observed that some differences exist in the specific year's cycle due to different pollution loads and annual variations of the water temperature and solar radiation and others in the year. In 1988, a warm and sunny January and February resulted in higher chlorophyll-a concentration in the waters and then subsequent overcast March postponed the spring algae bloom until April 1988. Sufficient solar radiation and available nutrients may result in higher chlorophyll-a and DO concentrations at the inner harbour near the end of year, e.g., in December 1988.

CONCLUSIONS

Simulation of phytoplankton growth in a coastal water system is complicated by many factors. A number of chemical, biological and biochemical processes interact and the reaction rates vary with time. External inputs and other parameters further complicate the time-varied nature of the phytoplankton population in the system. In addition, the flow and associated circulation are also functions of time, with time scale ranging from minutes to months, or even years. In this paper, a numerical model has been calibrated and verified with a long-term time-series monitoring data available in the Tolo Harbour, Hong Kong. The computational results agree with the measurements fairly well, i.e., the present model reproduces the unsteady two-layered eutrophication phenomena in the harbour successfully, and it is feasible to predict the eutrophication potentials and the effects of management activities, e.g., seasonal nutrients control, etc., by the model. It is anticipated that much better simulations will be obtained by the present model when more accurate pollution source data, including the point-sources, non-point-sources and atmospheric loads carried by rain and wind directly to the water surface are available.

ACKNOWLEDGEMENT

This project was supported by a grant from the Research Grant Committee of the University Grant Council of Hong Kong.

REFERENCES

Boers Paul C.M. and van der Molen Diederik T. (1993). Control of eutrophication in lakes: the state of the art in Europe, *European Water Pollution Control,* 3(2), pp. 19-2'5.

Cerco Carl F. and Cole Thomas. (1993). Three-Dimensional eutrophication model of Chesapeake Bay, *Journal of Environmental Engineering, ASCE,* 119(6), pp. 1006-1025.

Chau, K.W. and Jin, H.S. (1995). Numerical Solution of Two-layer, two-dimensional Tidal Flow in a Boundary Fitted Orthogonal Curvilinear Coordinate System*, International Journal for Numerical Methods in Fluids*, 21(11), pp. 1087-1107.

Chau, K.W. and Jin, H.S. (1999). Depth-averaged, two-dimensional eutrophication modelling for Tolo Harbour, Hong Kong, *Environmental Modeling and Assessment*, Vol. 4, pp. 189-199.

Chau, K.W. and Sin, Y.S. (1992). Correlation of Water Quality Parameters in Tolo Harbour, Hong Kong, *Water Science & Technology*, 26(9-11), pp. 2555-2558.

Environmental Protection Department, Hong Kong Government. (1990). *Marine water quality in Hong Kong results from the EPD marine water quality monitoring programme for 1989.* EP/TR 3/90.

Lung Wu-seng, Martin James L. and McCutcheon Steve C. (1993). Eutrophication analysis of embayments in Prince William Sound, Alaska, *Journal of Environmental Engineering, ASCE,* 119(5), pp. 8 1 1-824.

Patankar, S. V. (1980). *Numerical Heat Transfer and Fluid Flow,* Hemisphere Publishing Corporation.

Rodi, W. (1980). *Turbulence Models and Their Application in Hydraulics, state-of-the-art,* IAHR Publication, DELFT, The Netherlands.

Sin, Y. S. and Chau, K. W. (1992). Eutrophication studies on Tolo Harbour, Hong Kong, *Water Science and Technology,* 26(9-11), pp. 2551-2554.

Thomann, R.V. and Mueller, J.A. (1987). *Principles of Surface Water Quality Modeling and Control* Harper & Row, Publishers, New York.

Table 1. Kinetic parameters used in the 2-L, 2-D eutrophication model

PARAMETER	VALUE (AND θ)
Maximum phytoplankton growth rate	2.10 (1.066)
Half-saturation constant for nitrogen uptake	15.0
Half-saturation constant for phosphorus uptake	1.50
Endogenous respiration rate of phytoplankton	0.05 (1.08)
Nonpredatory mortality rate of phytoplankton	0.10
Grazing rate of zooplankton	0.30 (1.066)
Endogenous respiration rate of zooplankton	0.02 (1.045)
Mortality rate of zooplankton	0.10
Assimilated carbon per unit algae mass ingested (average CCHL)	112.5
Zooplankton assimilation efficiency	0.6
Half-maximum-efficiency food level for zooplankton filtering	12.0
Conversion efficiency of organic nitrogen to ammonia nitrogen	0.05 (1.08)
Stoichiometric ratio of cell nitrogen to algae chlorophyll-a	10.0
Stoichiometric ratio of cell nitrogen to zooplankton carbon	α_{13}/CCHL
Nitrification rate of ammonia to nitrate via nitrite nitrogen	0.05 (1.08)
Denitrification rate	0.09 (1.045)
Conversion efficiency of organic phosphorus to inorganic one	0.03 (1.08)
Stoichiometric ratio of phosphorus to algae chlorophyll-a	1.00
Stoichiometric ratio of phosphorus to zooplankton carbon	α_{16}/CCHL
Deoxygenation or decay rate of carbonaceous BOD	0.23 (1.047)
Ratio of the ultimate to 5-day carbonaceous BOD	1.54
Stoichiometric ratio of phytoplankton to organic carbon	CCHL
Stoichiometric ratio of zooplankton to organic carbon	1.00
Oxygen to nitrogen ratio	2.28
Stoichiometric ratio of phytoplankton to oxygen	2.67CCHL
Stoichiometric ratio of zooplankton to oxygen	$2.67\alpha_{28}$
O_2 consumed by per unit ammonia nitrogen stabilized	4.57
Fraction of dead algae and zoopl. recycled to organic nitrogen	0.50
Fraction of dead algae and zoopl. recycled to organic phosphorus	0.50
Fraction of dissolved organic nitrogen in total one	0.55
Fraction of dissolved organic phosphorus in total one	0.55
Fraction of dissolved orthophosphate in total one	0.75
Half saturation constant for phytoplankton affects mineralization	10.0
Half saturation DO constant for oxygen limitation of nitrification	2.0
Half-max. DO constant for oxygen limitation of denitrification	0.1
Half saturation DO constant for CBOD deoxygenation.	0.5
Settling rate of phytoplankton	1.10
Settling rate of zooplankton	0.0
Settling rate of particulate organic nitrogen	0.30
Settling rate of particulate organic phosphorus	0.30
Settling rate of othophosphate phosphorus sorbed	0.40
Settling rate of particulate CBOD	0.0

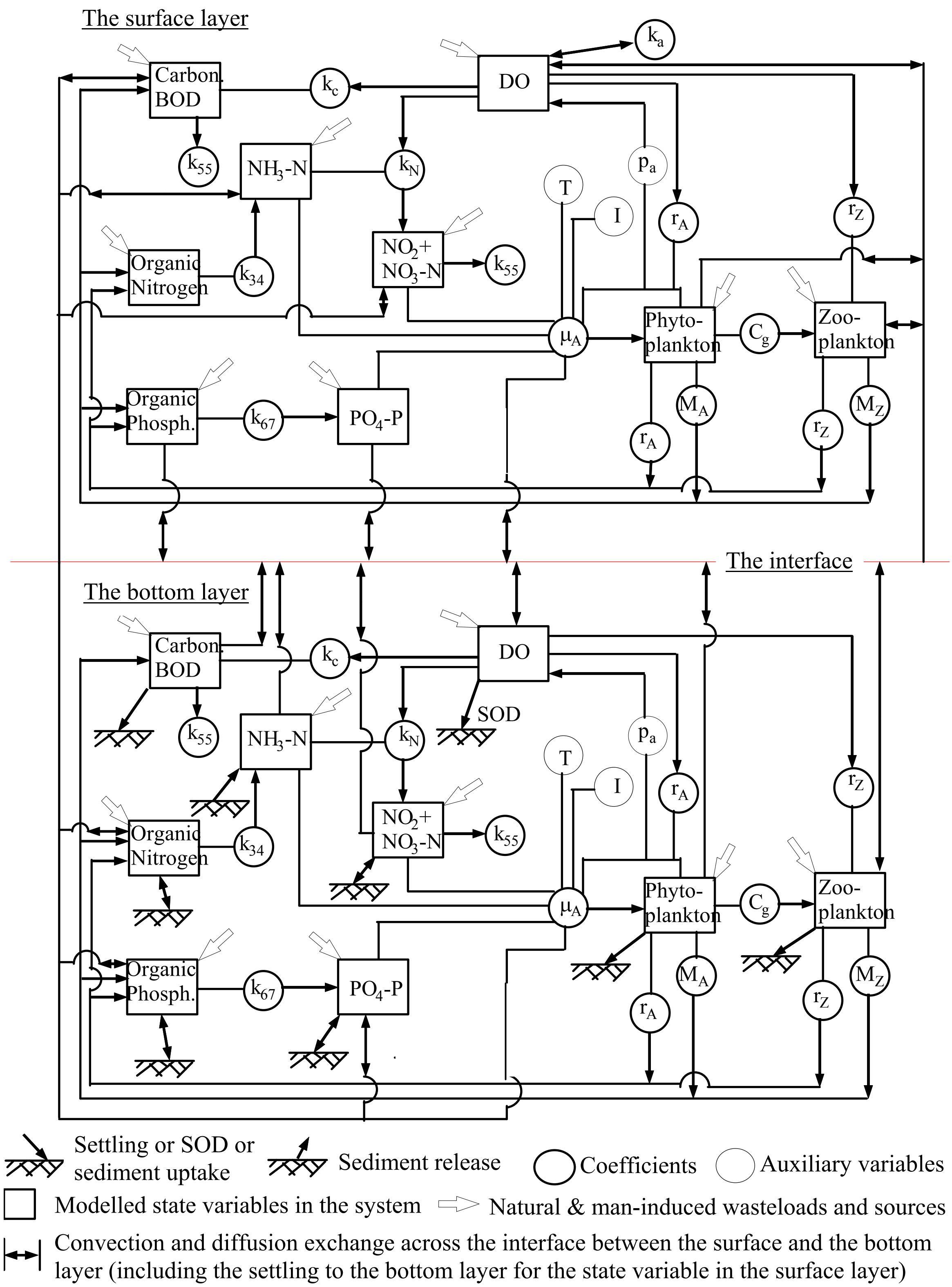

Fig.1 State variable interactions in the two-layered eutrophication model system

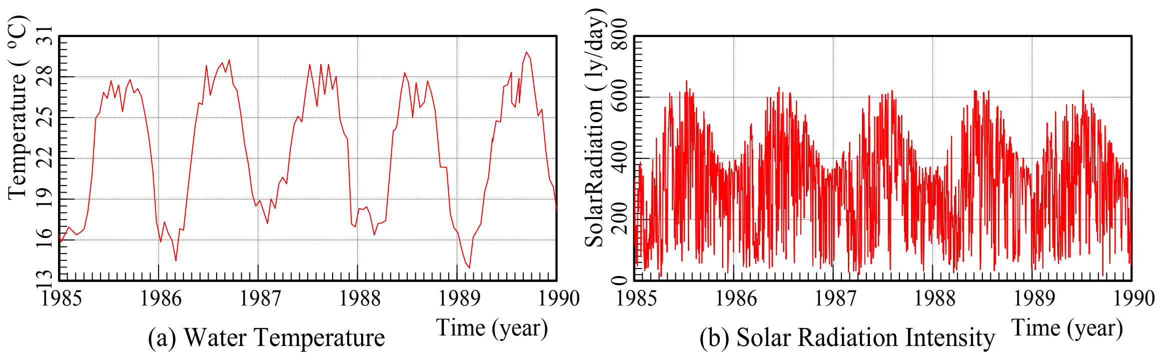

Fig. 2 Spatially-averaged surface water temperature and daily solar radiation in Tolo Harbour, Hong Kong

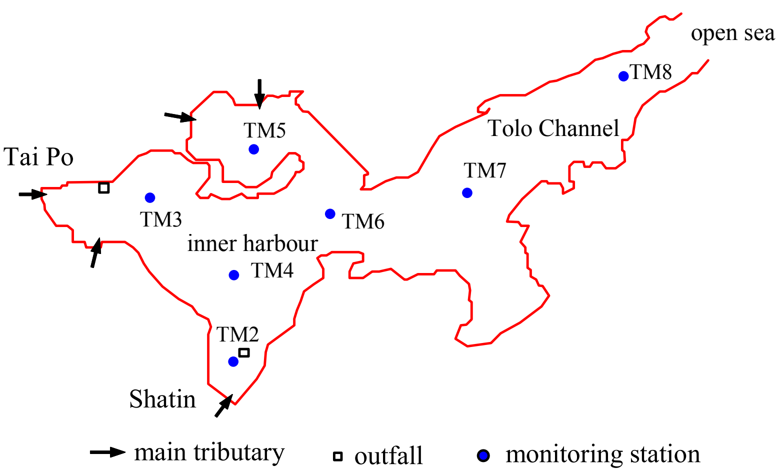

Fig. 3 Tolo Harbour in Hong Kong

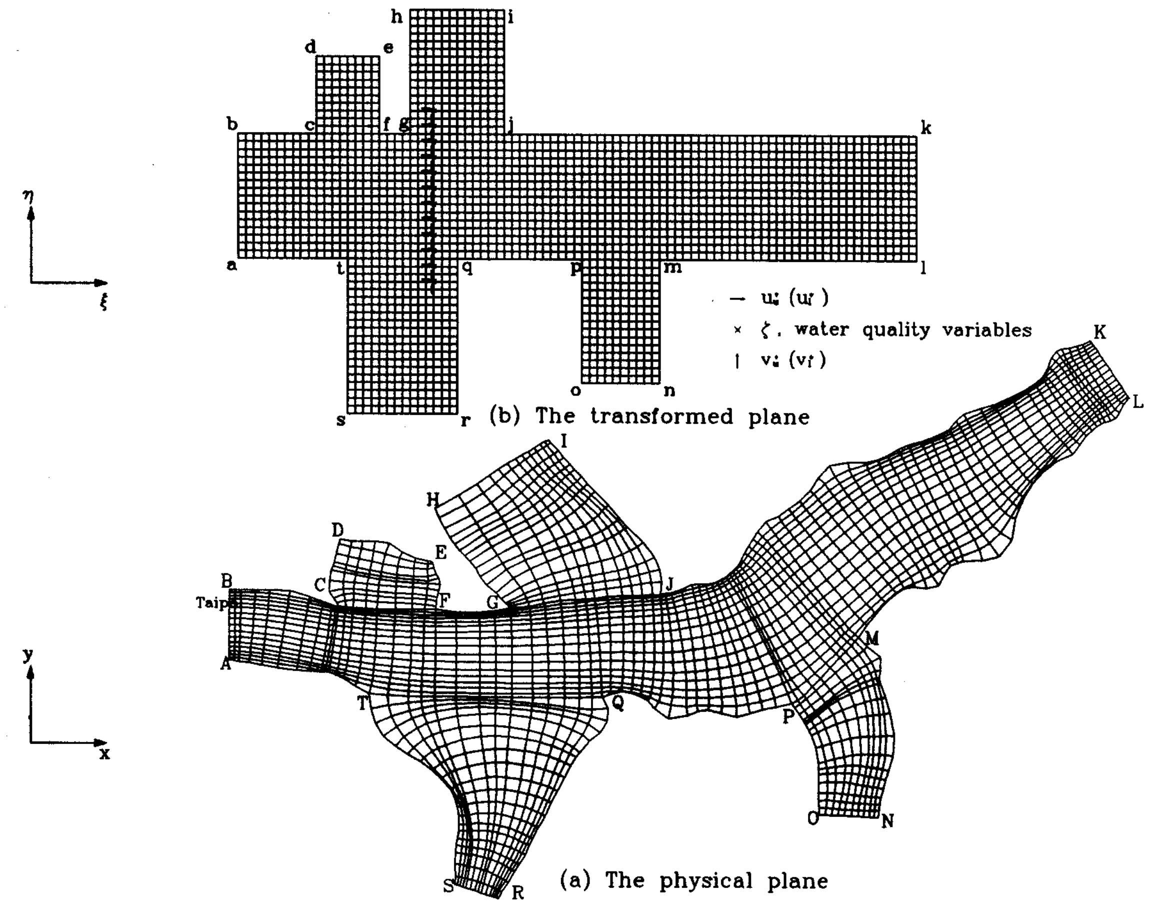

Fig. 4 Boundary-fitted curvilinear grid system: (a) physical plane; (b) transformed plane

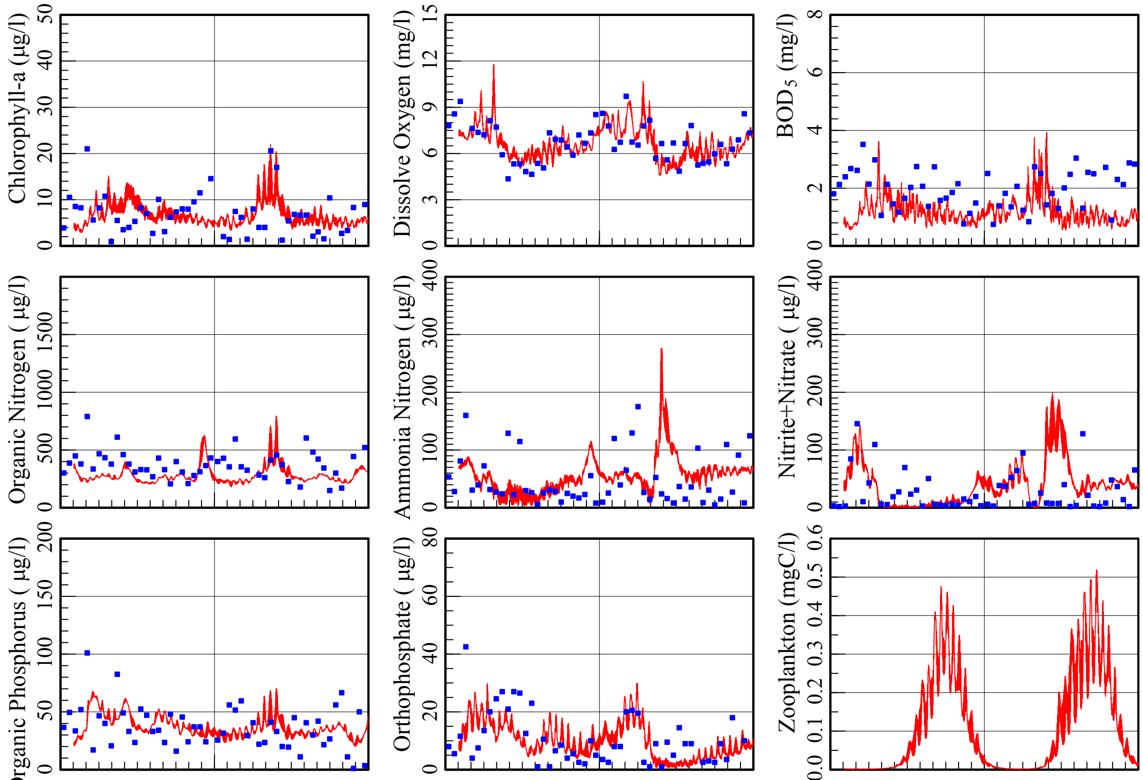

(1) In the surface layer

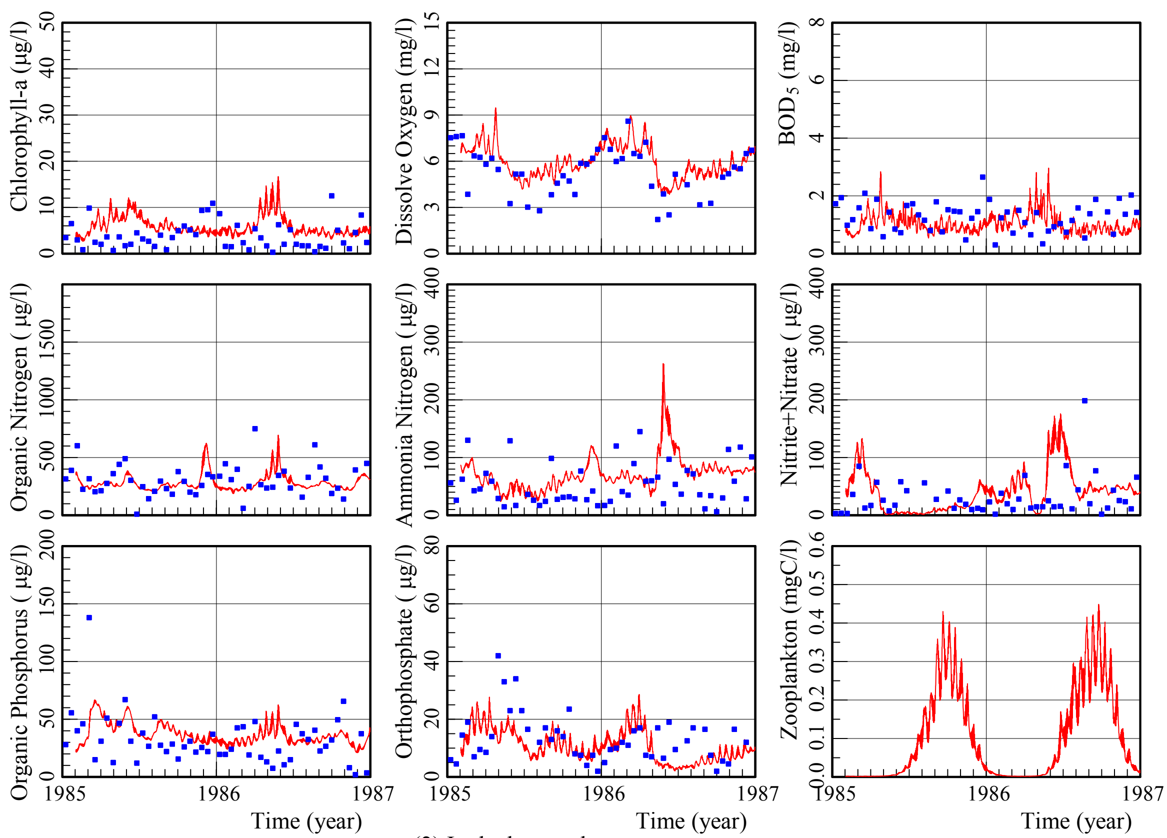

(2) In the bottom layer

Fig.5 Long-term time-series comparisons of results computed with the two-layered model and measured at TM6 in Tolo Harbour, Hong Kong, during 1985~1986 (— computed, ▪ measured)

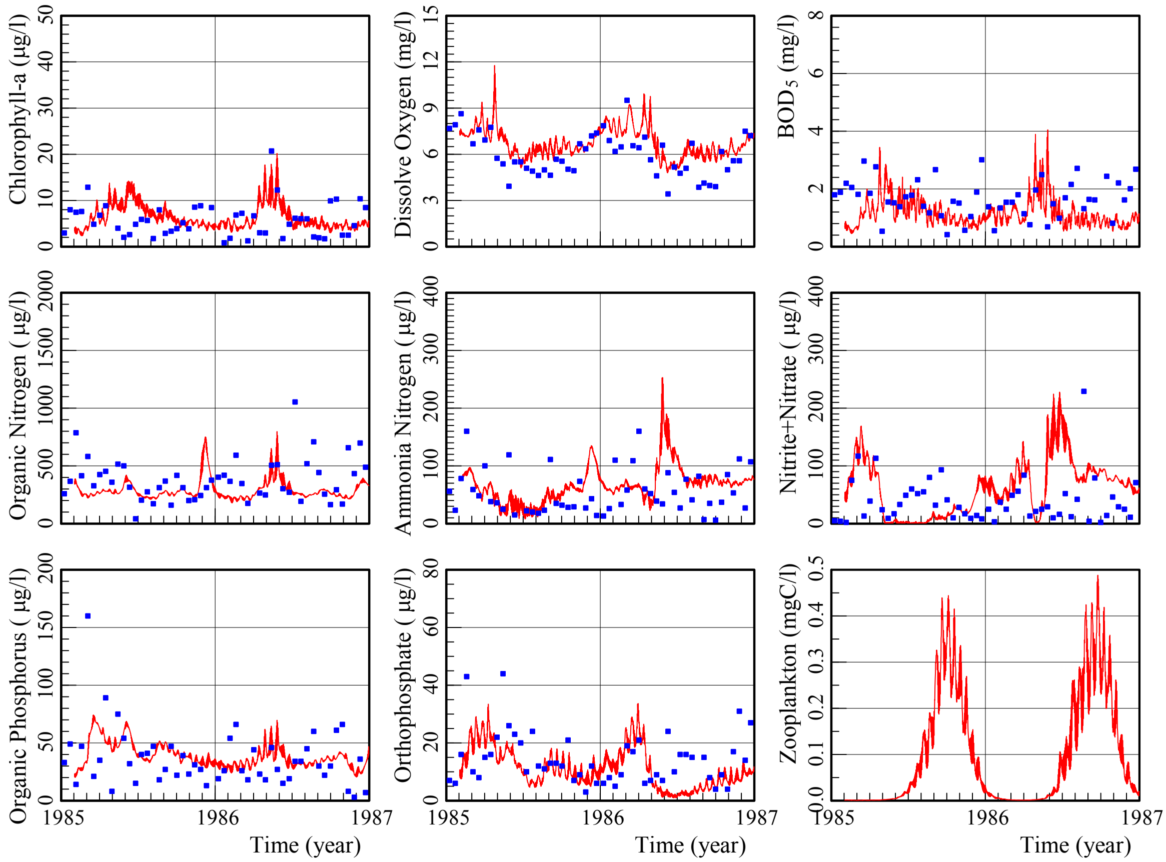

Fig.6 Long-term time-series comparisons of results computed with a depth-averaged model and measured at TM6 in Tolo Harbour, Hong Kong, during 1985~1986 (— computed, ▪ measured)

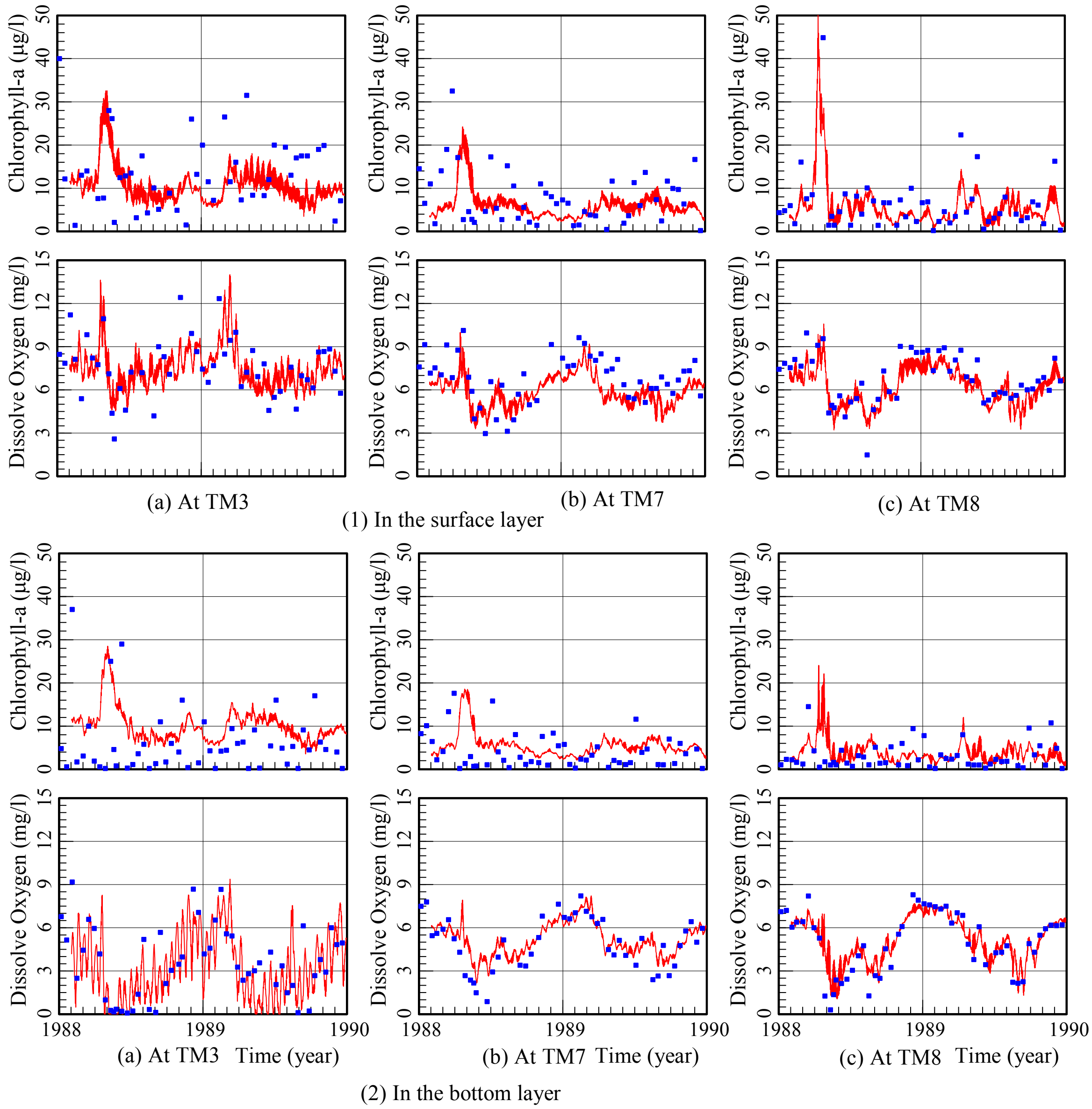

Fig.7 Chlorophyll-a and Dissolved Oxygen computed with the two-layered model and measured at different locations in Tolo Harbour, Hong Kong, during 1988~1990 (— computed, ▪ measured)

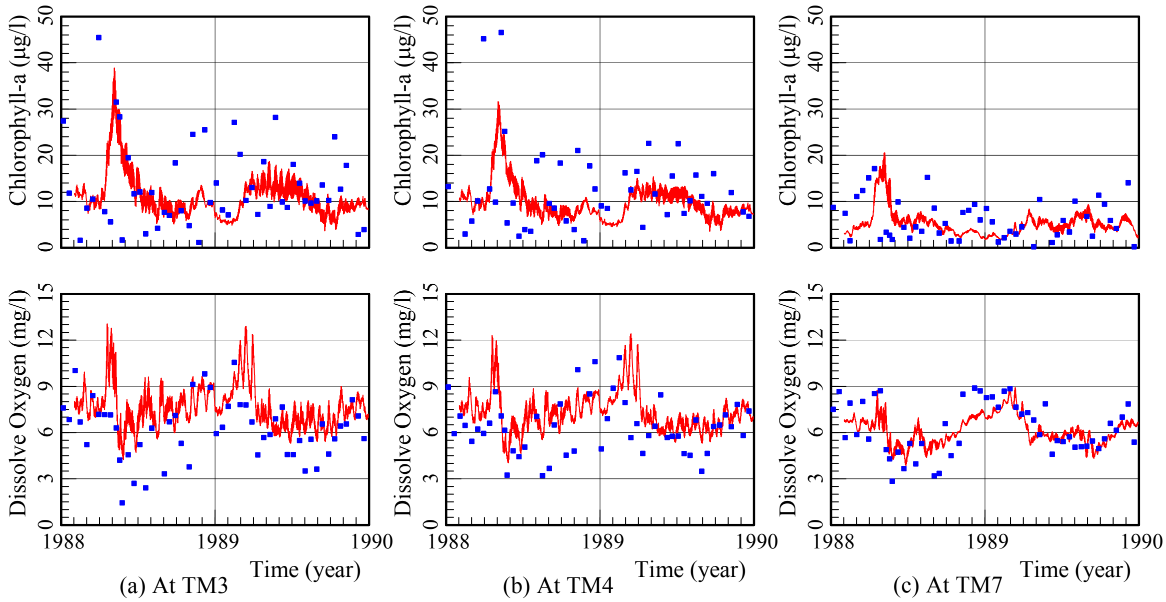

Fig.8 Chlorophyll-a and Dissolved Oxygen computed with a depth-averaged model and measured at different locations in Tolo Harbour, Hong Kong, during 1988~1990 (— computed, ▪ measured